On the Definition of Precipitation Efficiency

CHUNG-HSIUNG SUI

Institute of Hydrological Sciences, and Department of Atmospheric Sciences, National Central University, Jhongli City, Taiwan

XIAOFAN LI

Joint Center for Satellite Data Assimilation, and NOAA/NESDIS/Center for Satellite Applications and Research, Camp Springs, Maryland

MING-JEN YANG

Institute of Hydrological Sciences, National Central University, Jhongli City, Taiwan

(Manuscript received 26 October 2006, in final form 14 March 2007)

ABSTRACT

A modified definition of precipitation efficiency (PE) is proposed based on either cloud microphysics precipitation efficiency (CMPE) or water cycling processes including water vapor and hydrometeor species [large-scale precipitation efficiency (LSPE)]. These PEs are examined based on a two-dimensional cloud-resolving simulation. The model is integrated for 21 days with the imposed large-scale vertical velocity, zonal wind, and horizontal advections obtained from the Tropical Ocean Global Atmosphere Coupled Ocean–Atmosphere Response Experiment (TOGA COARE). It is found that the properly defined PEs include all moisture and hydrometeor sources associated with surface rainfall processes so that they range from 0% to 100%. Furthermore, the modified LSPE and CMPE are highly correlated. Their linear correlation coefficient and root-mean-squared difference are insensitive to the spatial scales of averaged data and are moderately sensitive to the time period of averaged data.

1. Introduction

Precipitation is directly produced by cloud microphysics processes at convective temporal and spatial scales. But the occurrence of precipitation is associated with environmental dynamics and thermodynamics of weather and climate events. So precipitation can be simply assumed to be proportional to the condensation rate (microphysical view) or the moisture flux in the convective systems (large-scale view). However, due to reevaporation of rain and local atmospheric moistening, not all condensation or moisture fluxes are used to produce precipitation. Therefore, precipitation efficiency is defined to evaluate how efficiently the convective system produces precipitation. This quantity is a crucial factor in a number of research topics. For example, precipitation efficiency is a key parameter in the closure assumptions in some cumulus parameterization schemes (Kuo 1965, 1974; Fritsch and Chappell 1980; Kain and Fritsch 1993; Grell 1993). Doswell et al. (1996) proposed an ingredient approach to forecasting the potential for heavy rainfall and flash floods using the precipitation efficiency as an essential conversion rate. In addition to the weather-scale topics, precipitation efficiency is also an important parameter for cloud–climate feedback processes. For example, Lau and Wu (2003) analyzed satellite data from the Tropical Rainfall Measuring Mission (TRMM; Simpson et al. 1988) and found that there is a substantial increase in precipitation efficiency of light warm rain as the sea surface temperature (SST) increases, but precipitation efficiency of heavy rain associated with deep convection is independent of sea surface temperature. This implies that in a warmer climate, there may be more warm rain at the expense of less cloud water available for mid- and high-level clouds. The dependence of precipitation efficiency on environmental warming is a key issue for the climate change study.

Corresponding author address: C.-H. Sui, Institute of Hydrological Sciences, National Central University, No. 300, Wu-Chuan Li, Jhongli City, Taoyuan, 320, Taiwan.
E-mail: sui@ncu.edu.tw

DOI: 10.1175/2007JAS2332.1

Because of its fundamental importance, the precipitation efficiency of convective storms has been estimated in many studies in the past five decades (Braham 1952). Precipitation efficiency can be defined as the ratio of the surface rain rate to the sum of vapor convergence and surface evaporation rates, or large-scale precipitation efficiency (LSPE; e.g., Auer and Marwitz 1968; Heymsfield and Schotz 1985; Chong and Hauser 1989; Doswell et al. 1996; Ferrier et al. 1996; Li et al. 2002a; Tao et al. 2004; Sui et al. 2005). The LSPE has been used mostly in observational studies, since the vapor convergence and surface evaporation can be calculated from the sounding and field experiment data. Precipitation efficiency can also be defined as the ratio of the surface rain rate to the sum of vapor condensation and deposition rates, or cloud microphysics precipitation efficiency (CMPE; e.g., Weisman and Klemp 1982; Lipps and Hemler 1986; Ferrier et al. 1996; Li et al. 2002a; Sui et al. 2005). The CMPE, on the other hand, is examined mainly in cloud modeling studies, because the vapor condensation and deposition rates can be produced during the model integration.

Despite these efforts, precipitation efficiency remains to be defined properly and to be calculated accurately. For example, both LSPE and CMPE could be greater than 100% and LSPE could be negative (e.g., Fig. 4 in Sui et al. 2005). What causes these physically unreasonable precipitation efficiencies? How should precipitation efficiency be defined and calculated properly? These are the key questions we want to address in this paper. We shall demonstrate that despite different aspects, LSPE and CMPE are fundamentally the same based on physical considerations; hence, in the present study we shall investigate the statistical equivalence between LSPE and CMPE in the tropical convective regime for different spatial and temporal scales.

In this paper, the definitions of precipitation efficiency will be discussed using the two-dimensional cloud-resolving model simulation data during the Tropical Ocean Global Atmosphere Coupled Ocean–Atmosphere Response Experiment (TOGA COARE). In next section, the cloud model and forcing are briefly introduced and experiments are described. The LSPE and CMPE are discussed in sections 3 and 4, respectively. The new precipitation efficiencies are compared in section 5. The summary is given in section 6.

2. Model and experiment designs

The cloud-resolving model used in this study was originally developed by Soong and Ogura (1980), Soong and Tao (1980), and Tao and Simpson (1993). The 2D version of the model used by Sui et al. (1994, 1998) and further modified by Li et al. (1999) is what is used in this study. The governing equations and model setup can be found in Li et al. (1999, 2002b). The cloud-resolving simulations have been validated with observations in terms of atmospheric thermodynamic profiles, surface fluxes, and surface rain rates in the Tropics during the Global Atmospheric Research Programme Atlantic Tropical Experiment (GATE; e.g., Xu and Randall 1996; Grabowski et al. 1996) and TOGA COARE (e.g., Wu et al. 1998; Li et al. 1999, 2002a,b).

The model is forced by zonally uniform vertical velocity, zonal wind, and thermal and moisture advection based on 6-hourly TOGA COARE observations within the Intensive Flux Array (IFA) region (M. Zhang 1999, personal communication). The calculations are based on a constrained, variational method applied to column-integrated budgets of mass, heat, moisture, and momentum as proposed by Zhang and Lin (1997). Hourly sea surface temperature at the Improved Meteorological (IMET) surface mooring buoy (1.75°S, 156°E; Weller and Anderson 1996) is also imposed in the model. The model is integrated from 0400 local standard time (LST) 18 December 1992 to 1000 LST 9 January 1993 (21.25 days total). Figure 1 shows the time evolution of the vertical distribution of the large-scale vertical velocity and zonal wind and the time series of the SST, which are imposed in the model during the integrations. In the model setup, the horizontal boundary is periodic. The horizontal domain is 768 km with a grid resolution of 1.5 km. The vertical grid resolution ranges from about 200 m near the surface to about 1 km near 100 mb. The time step is 12 s. Hourly 96-km-mean simulation data are used in the following analysis unless the data are indicated otherwise.

3. Cloud microphysics precipitation efficiency

Sui et al. (2005) defined the following precipitation efficiency based on the hydrometeor budget:

$$\mathrm{CMPE1} = \frac{P_s}{[\mathrm{SI}_{qv}]} = 1 - \frac{[\mathrm{SO}_{qv}]}{[\mathrm{SI}_{qv}]} + \frac{[\mathrm{CONV}_C]}{[\mathrm{SI}_{qv}]}. \quad (1)$$

Here a square bracket denotes a vertically integrated quantity ($[F] = \int_0^{z_t} \bar{\rho} F\, dz$ for any variable F and z_t is the model top); P_s is the surface rainfall rate; $\mathrm{SI}_{qv} = [P_{\mathrm{CND}}] + [P_{\mathrm{DEP}}] + [P_{\mathrm{SDEP}}] + [P_{\mathrm{GDEP}}]$ represents the sink term in the water vapor budget that consists of vapor condensation rate ($[P_{\mathrm{CND}}]$), vapor deposition rates for the growth of cloud ice ($[P_{\mathrm{DEP}}]$), snow ($[P_{\mathrm{SDEP}}]$), and graupel ($[P_{\mathrm{GDEP}}]$); and $\mathrm{SO}_{qv} = [P_{\mathrm{REVP}}] + [P_{\mathrm{MLTG}}] + [P_{\mathrm{MLTS}}]$ represents the source term consisting of the growth of vapor by evaporation of raindrops ($[P_{\mathrm{REVP}}]$), melting graupel ($[P_{\mathrm{MLTG}}]$), and melting snow ($[P_{\mathrm{MLTS}}]$).

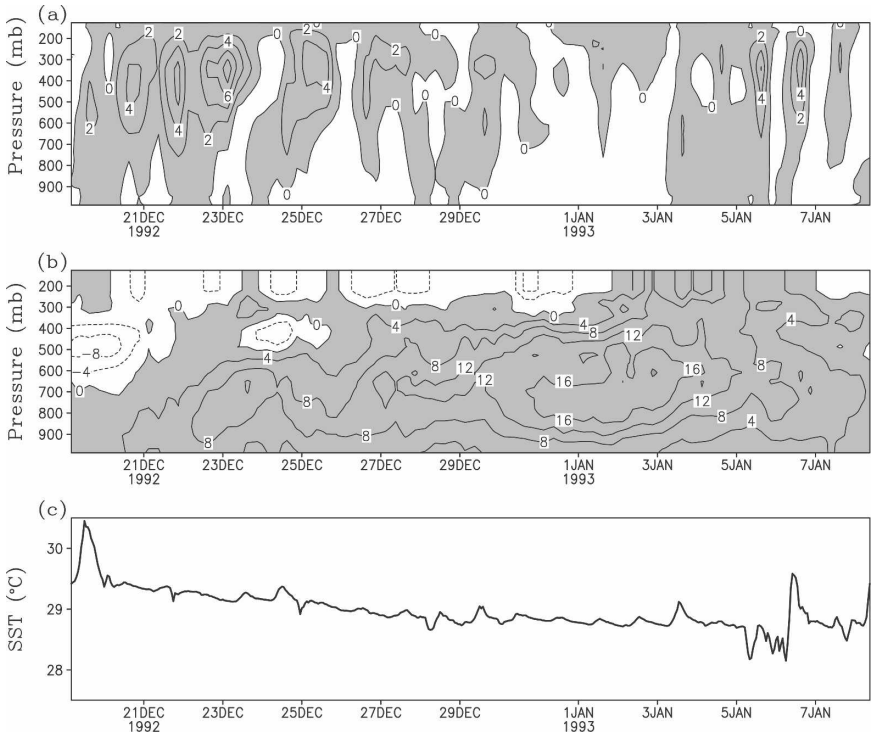

FIG. 1. Temporal and vertical distribution of (a) vertical velocity, (b) zonal wind, and (c) time series of SST observed and derived from TOGA COARE for the 21-day period. Upward motion in (a) and westerly wind in (b) are shaded. Units of vertical velocity, zonal wind, and SST are cm s^{-1}, m s^{-1}, and °C, respectively.

The $[\mathrm{CONV}_C]$ is the convergence of hydrometeor $C = q_5 = q_c + q_r + q_i + q_s + q_g$, where q_c, q_r, q_i, q_s, and q_g are the mixing ratios of cloud water (small cloud droplets), raindrops, cloud ice (small ice crystals), snow (density = 0.1 g cm^{-3}), and graupel (density = 0.4 g cm^{-3}), respectively.

The above definition of CMPE1 in Eq. (1), however, does not include all source terms for the eventual formation of surface precipitation. This can be seen in the hydrometeor budget equation, $\partial[C]/\partial t = [\mathrm{CONV}_C] - P_s + \mathrm{SI}_{qv} - \mathrm{SO}_{qv}$; the term $-\partial[C]/\partial t + [\mathrm{CONV}_C]$ may contribute to surface precipitation if they are positive. To count all hydrometeor sources for precipitation, a more complete precipitation efficiency is defined as

$$\mathrm{CMPE2} = \frac{P_s}{[P_{\mathrm{CND}}] + [P_{\mathrm{DEP}}] + [P_{\mathrm{SDEP}}] + [P_{\mathrm{GDEP}}] + \mathrm{sgn}(Q_{\mathrm{CM}})Q_{\mathrm{CM}}}, \tag{2}$$

where

$$\mathrm{sgn}(F) = 1, \quad \text{when} \quad F > 0; \quad \mathrm{sgn}(F) = 0, \quad \text{when} \quad F \le 0; \tag{2a}$$

and

$$Q_{\mathrm{CM}} = -\partial[C]/\partial t + [\mathrm{CONV}_C]. \tag{2b}$$

Here Q_{CM} is the sum of local hydrometeor change and hydrometeor convergence.

Figure 2 shows CMPE1 versus CMPE2, using hourly 96-km averaged data during the 21-day integration. CMPE1 ranges from 0% to 350%, whereas CMPE2 is between 0% and 100% as expected when all sources associated with rainfall in cloud microphysical budgets are counted in the calculations of CMPE. Figure 3 displays CMPE1 and CMPE2 as functions of P_s. For strong rainfall ($P_s > 5$ mm h^{-1}), both CMPE1 and CMPE2 range from 50% to 100%. For weak rainfall ($P_s < 5$ mm h^{-1}), CMPE1 ranges from 0% to 350%. The fact that large CMPE1 appears when P_s is small (Fig. 3a) suggests that CMPE1 is sensitive to rainfall sources Q_{CM} during light rains. Both CMPE1 and CMPE2 have a tendency to converge to a finite value as P_s increases (Fig. 3b).

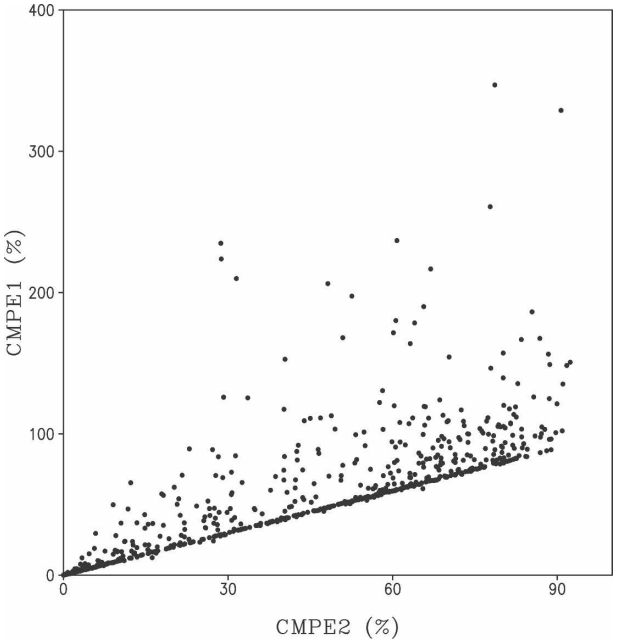

FIG. 2. CMPE1 (%) vs CMPE2 (%) using hourly 96-km averaged data during the 21-day integration.

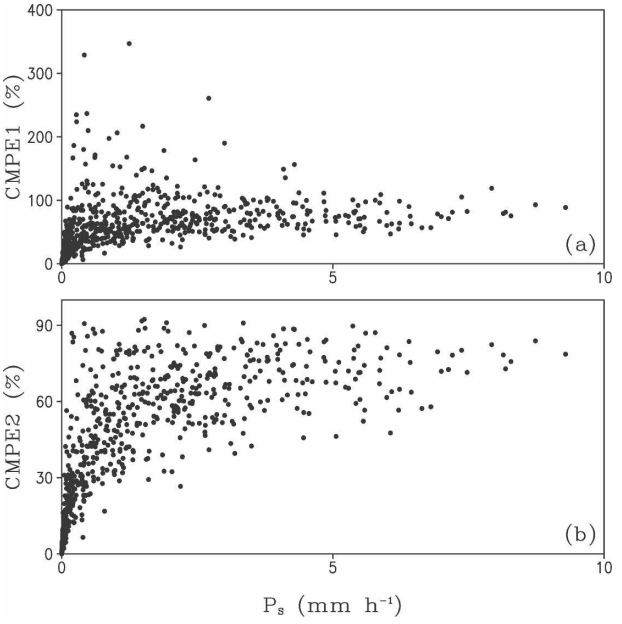

FIG. 3. (a) CMPE1 (%) vs P_s (mm h^{-1}) and (b) CMPE2 vs P_s using hourly 96-km averaged data during the 21-day integration.

4. Large-scale precipitation efficiency

From the water vapor budget, $\partial[q_v]/\partial t = [\mathrm{CONV}_{qv}] + E_s - \mathrm{SI}_{qv} + \mathrm{SO}_{qv}$, combined with the hydrometeor budget, Gao et al. (2005) derived a surface rainfall equation, which can be expressed by

$$P_s = Q_{\mathrm{WVT}} + Q_{\mathrm{WVF}} + Q_{\mathrm{WVE}} + Q_{\mathrm{CM}}, \tag{3}$$

where Q_{WVT} ($= -\partial[q_v]/\partial t$) is the local vapor change, Q_{WVF} is vapor convergence $[\mathrm{CONV}_{qv}]$, Q_{WVE} is the surface evaporation rate, and Q_{CM} is the sum of local hydrometeor change and hydrometeor convergence defined in Eq. (2). Based on Eq. (3), the following precipitation efficiency originally defined in Sui et al. (2005),

$$\mathrm{LSPE1} = \frac{P_s}{[\mathrm{CONV}_{qv}] + E_s} = \frac{P_s}{Q_{\mathrm{WVF}} + Q_{\mathrm{WVE}}}, \tag{4}$$

neglects the possible contributions by the source terms of Q_{WVT} and Q_{CM} when they are positive. We note here that while Q_{WVE} is always a rainfall source because it is positive, Q_{WVT}, Q_{WVF}, and Q_{CM} may not be rainfall sources when they are negative. Generally speaking, local vapor loss ($Q_{\mathrm{WVT}} > 0$), vapor convergence ($Q_{\mathrm{WVF}} > 0$), local hydrometeor loss, and hydrometeor convergence ($Q_{\mathrm{CM}} > 0$) all contribute to the formation of surface rainfall. Thus, a new LSPE based on Eq. (3) is defined as

$$\mathrm{LSPE2} = \frac{P_s}{\sum_{i=1}^{4} \mathrm{sgn}(Q_i) Q_i}, \tag{5}$$

where $Q_i = (Q_{\mathrm{WVT}}, Q_{\mathrm{WVF}}, Q_{\mathrm{WVE}}, Q_{\mathrm{CM}})$.

Figure 4 shows the scatterplot of LSPE1 against LSPE2. The figure shows that not only can LSPE1 be larger than 100%, but it can also be negative such that its values range from −500% to 500%. On the other hand, LSPE2 ranges between 0% and 100%. Clearly, including all vapor and hydrometeor sources associated with surface rainfall in LSPE2 eliminates all negative values and values larger than 100%. A further examination of LSPE1 and LSPE2 as functions of P_s in Fig. 5 shows that LSPE2 tends to increase with increasing P_s such that the range of LSPE2 narrows with increasing P_s. On the other hand, values of LSPE1 have a much wider range of variability than those of LSPE2 and converge to a finite value with increasing P_s. Figure 5 also shows that negative values of LSPE1 correspond to weak rainfall condition ($P_s < 5$ mm h^{-1}).

The definition of LSPE2 in Eq. (5) shows that LSPE2 is a function of cloud source/sink (Q_{CM}). To examine the impacts of Q_{CM} on LSPE2, LSPE2 is calculated by setting Q_{CM} to be zero [LSPE2($Q_{\mathrm{CM}} = 0$)]. Figure 6 shows LSPE2($Q_{\mathrm{CM}} = 0$) versus LSPE2. LSPE2($Q_{\mathrm{CM}} = 0$) is generally larger than LSPE2, and could be larger

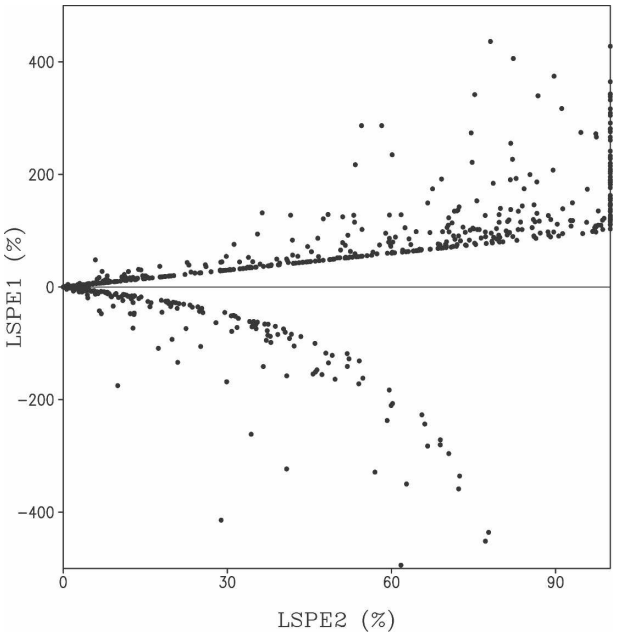

FIG. 4. LSPE1 (%) vs LSPE2 (%) using hourly 96-km averaged data during the 21-day integration.

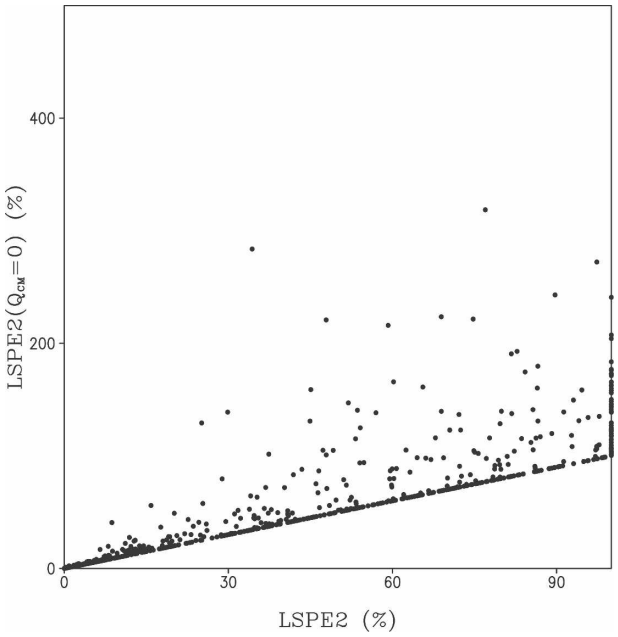

FIG. 6. LSPE2(Q_{CM} = 0) (%) vs LSPE2 (%) using hourly 96-km averaged data during the 21-day integration.

than 100%, especially when LSPE2 is larger (say, >50%).

LSPE1 may not be an appropriate precipitation efficiency because it may be negative, larger than 100%, and is unity for the large-scale average. LSPE2 could be a strong function of both water vapor and cloud hydrometeors, though it ranges between 0% and 100%. This suggests that CMPE may be a more appropriate parameter for the estimation of precipitation efficiency in cloud models.

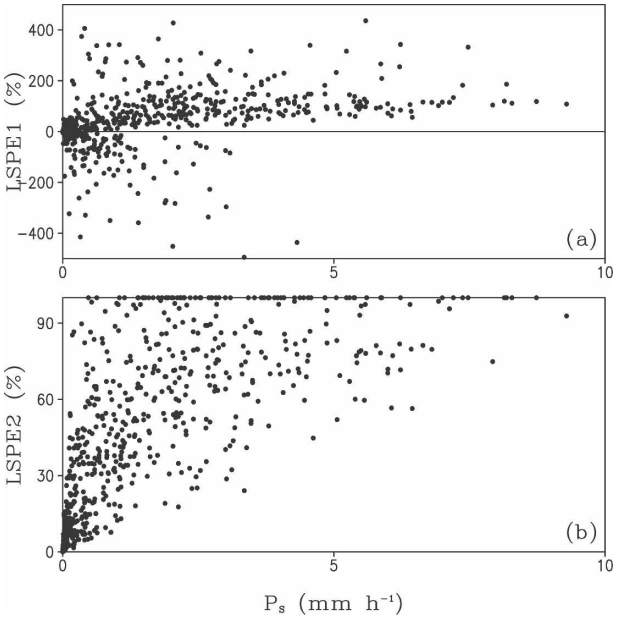

FIG. 5. (a) LSPE1 (%) vs P_s (mm h^{-1}) and (b) LSPE2 vs P_s using hourly 96-km averaged data during the 21-day integration.

5. CMPE2 versus LSPE2

Figure 7 shows CMPE2 versus LSPE2 using the hourly 96-km averaged data. The root-mean-squared (RMS) difference between CMPE2 and LSPE2 is 18.5%, which is smaller than the standard deviations of CMPE2 (28.5%) and LSPE2 (35.1%). The linear correlation coefficient between CMPE2 and LSPE2 is 0.85, which is well above the 1% significance level of 757 degrees of freedom in the Student's *t* test.

To examine the dependence of precipitation efficiency on temporal and spatial scales, LSPE2 and CMPE2 are calculated using 6-hourly mean and daily mean 96-km averaged data (Fig. 8) and hourly 48- and 24-km averaged data (Fig. 9), respectively. The linear correlation coefficients and RMS differences between CMPE2 and LSPE2 are 0.79% and 22.3% for 6-hourly mean 96-km averaged data, 0.70% and 23.4% for daily mean 96-km averaged data, 0.85% and 17.9% for hourly 48-km averaged data, and 0.84% and 17.8% for hourly 24-km averaged data, respectively. The results indicate that the linear correlation coefficient decreases and RMS difference increases as the time period of averaged data increases. Figure 8 shows that LSPE2 is larger than CMPE2 for higher values of precipitation

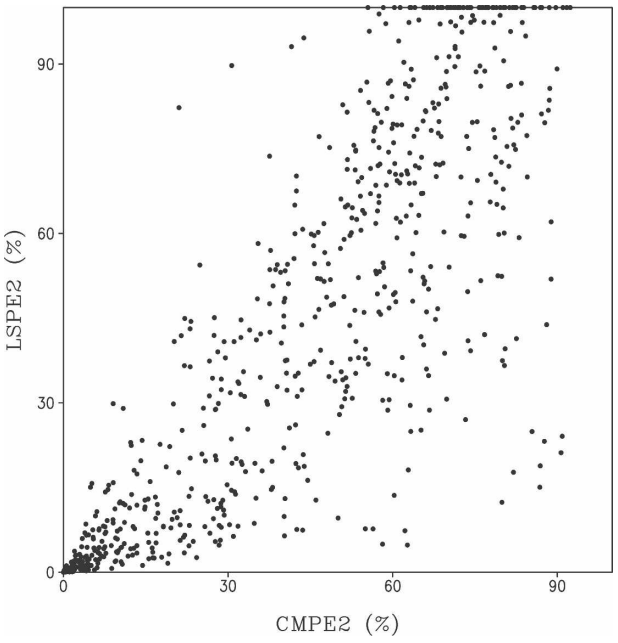

FIG. 7. LSPE2 (%) vs CMPE2 (%) using hourly 96-km averaged data during the 21-day integration.

efficiency, whereas it is the opposite for lower values of precipitation efficiency. The results in Fig. 9 further suggest that LSPE2 and CMPE2 are insensitive to spatial scales of averaged data.

6. Summary

Because of its importance in the closure of cumulus parameterization and prediction of heavy rainfall, the precipitation efficiency has been investigated in many studies in the past five decades. Some studies (e.g., Tao et al. 2004; Sui et al. 2005) show that precipitation efficiency may be larger than 100%. Such physically unreasonable values of precipitation efficiency arise due to the fact that sources associated with surface rainfall are not fully counted. The precipitation efficiency in the tropical convective regime is revisited in this study by analyzing a two-dimensional cloud-resolving model simulation. The model is forced by the imposed large-scale vertical velocity, zonal wind, and horizontal advections obtained from TOGA COARE data. The model is integrated for 21 days. More complete definitions of precipitation efficiency are proposed in this study based on either the moisture budget (LSPE2) or hydrometeor budget (CMPE2) that include all sources related to surface rainfall processes. The major results include

- LSPE2 and CMPE2 range from 0% to 100%.
- CMPE2 is only associated with cloud microphysical processes whereas LSPE2 is related to water cycling processes including both water vapor and hydrometeor species. LSPE2 and CMPE2 are highly correlated. Their linear correlation coefficient and root-mean-squared difference are moderately sensitive to the time period of averaged data, whereas they are not sensitive to the spatial scales of averaged data.
- Simplified precipitation efficiencies like LSPE1 and CMPE1 may be larger than 100% when some source

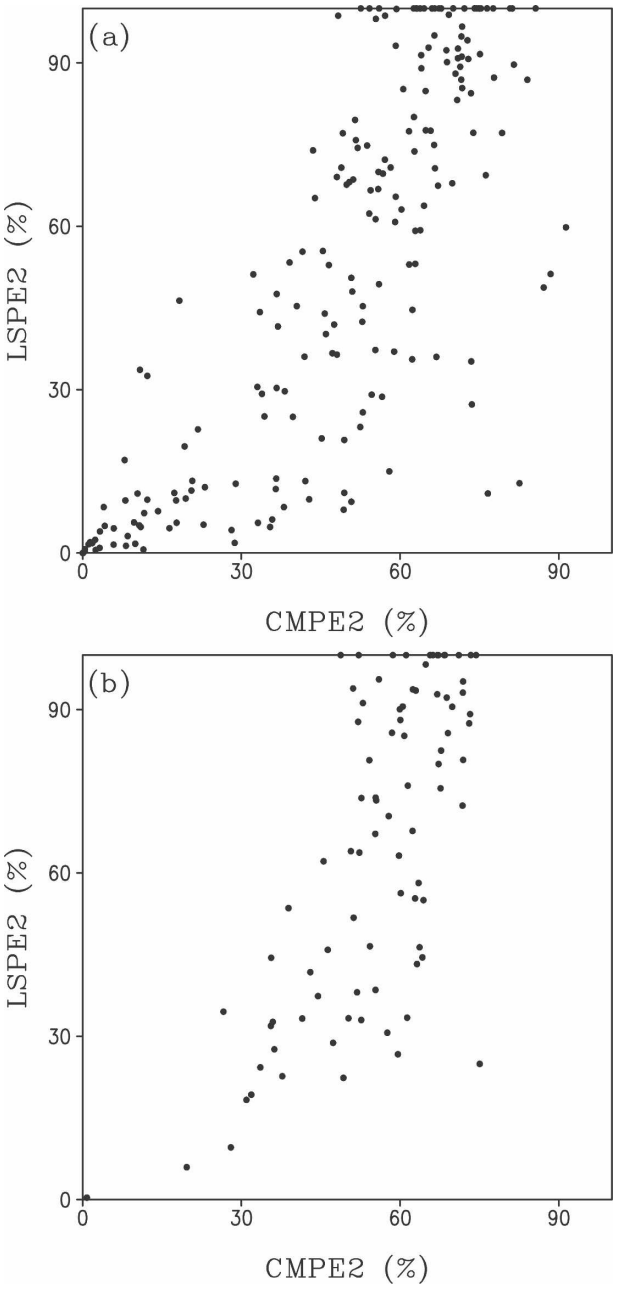

FIG. 8. LSPE2 (%) vs CMPE2 (%) using (a) 6-hourly mean and (b) daily mean 96-km averaged data during the 21-day integration.

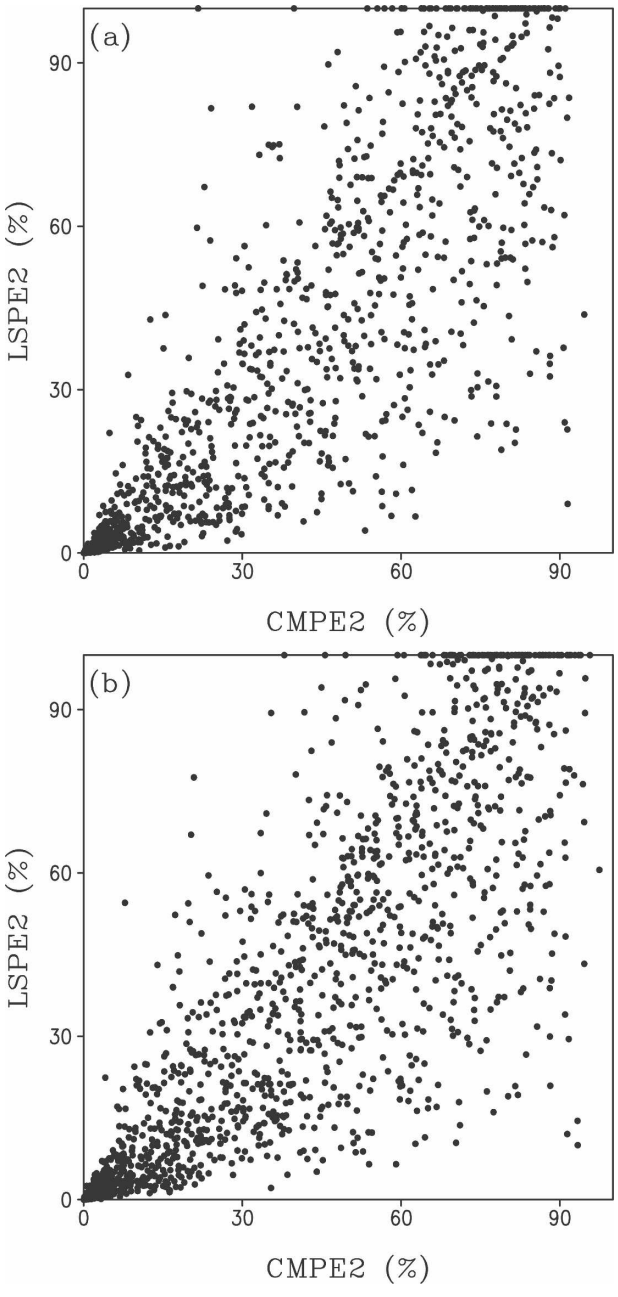

FIG. 9. LSPE2 (%) vs CMPE2 (%) using hourly (a) 48- and (b) 24-km averaged data during the 21-day integration.

terms are excluded in the calculations. This is more likely to occur in the light rain conditions when the contribution to the surface rain by local vapor change, local hydrometeor change, and hydrometeor convergence becomes significant. In the heavy rain conditions, the simplified precipitation efficiencies of LSPE1 and CMPE1 appear to be good enough measures of precipitation efficiency.

- CMPE2 (or CMPE1) is a physically more straightforward definition of precipitation efficiency than LSPE2 (or LSPE1). But the former can only be estimated in models with explicit parameterization of cloud microphysics, which is model-dependent, while the latter may be estimated based on currently available assimilation data of satellite and sounding measurements.

Some questions remain unanswered. For example, why does the precipitation efficiency of CMPE2 approach a constant threshold as P_s increases? Will the statistical equivalence between CMPE2 and LSPE2 still be valid for other precipitation regimes? Can we apply these efficiencies of CMPE2 and LSPE2 to a precipitating system with more three-dimensional structures? Further studies are needed to answer these questions.

Acknowledgments. The authors thank Dr. W.-K. Tao at NASA GSFC for his cloud-resolving model, Prof. M. Zhang at SUNY (Stony Brook) for his TOGA COARE forcing data, and reviewers for their constructive comments. This research has been supported by the National Sciences Council in Taiwan under Grants NSC 095-2111-M-008-003 and NSC 094-2111-M-008-008.

REFERENCES

Auer, A. H., Jr., and J. D. Marwitz, 1968: Estimates of air and moisture flux into hailstorms on the High Plains. *J. Appl. Meteor.,* **7,** 196–198.

Braham, R. R., Jr., 1952: The water and energy budgets of the thunderstorm and their relation to thunderstorm development. *J. Meteor.,* **9,** 227–242.

Chong, M., and D. Hauser, 1989: A tropical squall line observed during the COPT 81 experiment in West Africa. Part II: Water budget. *Mon. Wea. Rev.,* **117,** 728–744.

Doswell, C. A., III, H. E. Brooks, and R. A. Maddox, 1996: Flash flood forecasting: An ingredients-based methodology. *Wea. Forecasting,* **11,** 560–581.

Ferrier, B. S., J. Simpson, and W.-K. Tao, 1996: Factors responsible for precipitation efficiencies in midlatitude and tropical squall simulations. *Mon. Wea. Rev.,* **124,** 2100–2125.

Fritsch, J. M., and C. F. Chappell, 1980: Numerical prediction of convectively driven mesoscale pressure systems. Part I: Convective parameterization. *J. Atmos. Sci.,* **37,** 1722–1733.

Gao, S., X. Cui, Y. Zhou, and X. Li, 2005: Surface rainfall processes as simulated in a cloud-resolving model. *J. Geophys. Res.,* **110,** D10202, doi:10.1029/2004JD005467.

Grabowski, W. W., X. Wu, and M. W. Moncrieff, 1996: Cloud-resolving model of tropical cloud systems during Phase III of GATE. Part I: Two-dimensional experiments. *J. Atmos. Sci.,* **53,** 3684–3709.

Grell, G. A., 1993: Prognostic evaluation of assumptions used by cumulus parameterizations. *Mon. Wea. Rev.,* **121,** 764–787.

Heymsfield, G. M., and S. Schotz, 1985: Structure and evolution of a severe squall line over Oklahoma. *Mon. Wea. Rev.,* **113,** 1563–1589.

Kain, J. S., and J. M. Fritsch, 1993: Convective parameterization for mesoscale models: The Kain-Fritsch scheme. *The Repre-*

sentation of Cumulus Convection in Numerical Models, Meteor. Monogr., No. 46, Amer. Meteor. Soc., 165–177.

Kuo, H. L., 1965: On formation and intensification of tropical cyclones through latent heat release by cumulus convection. *J. Atmos. Sci.,* **22,** 40–63.

——, 1974: Further studies of the parameterization of the influence of cumulus convection on large-scale flow. *J. Atmos. Sci.,* **31,** 1232–1240.

Lau, K. M., and H. T. Wu, 2003: Warm rain processes over tropical oceans and climate implications. *Geophys. Res. Lett.,* **30,** 2290, doi:10.1029/2003GL018567.

Li, X., C.-H. Sui, K.-M. Lau, and M.-D. Chou, 1999: Large-scale forcing and cloud–radiation interaction in the tropical deep convective regime. *J. Atmos. Sci.,* **56,** 3028–3042.

——, ——, and ——, 2002a: Precipitation efficiency in the tropical deep convective regime: A 2-D cloud resolving modeling study. *J. Meteor. Soc. Japan,* **80,** 205–212.

——, ——, and ——, 2002b: Dominant cloud microphysical processes in a tropical oceanic convective system: A 2D cloud resolving modeling study. *Mon. Wea. Rev.,* **130,** 2481–2491.

Lipps, F. B., and R. S. Hemler, 1986: Numerical simulation of deep tropical convection associated with large-scale convergence. *J. Atmos. Sci.,* **43,** 1796–1816.

Simpson, J., R. F. Adler, and G. R. North, 1988: A proposed Tropical Rainfall Measuring Mission (TRMM) satellite. *Bull. Amer. Meteor. Soc.,* **69,** 278–295.

Soong, S.-T., and Y. Ogura, 1980: Response of tradewind cumuli to large-scale processes. *J. Atmos. Sci.,* **37,** 2035–2050.

——, and W.-K. Tao, 1980: Response of deep tropical cumulus clouds to mesoscale processes. *J. Atmos. Sci.,* **37,** 2016–2034.

Sui, C.-H., K.-M. Lau, W.-K. Tao, and J. Simpson, 1994: The tropical water and energy cycles in a cumulus ensemble model. Part I: Equilibrium climate. *J. Atmos. Sci.,* **51,** 711–728.

——, X. Li, and K.-M. Lau, 1998: Radiative–convective processes in simulated diurnal variations of tropical oceanic convection. *J. Atmos. Sci.,* **55,** 2345–2357.

——, ——, M.-J. Yang, and H.-L. Huang, 2005: Estimation of oceanic precipitation efficiency in cloud models. *J. Atmos. Sci.,* **62,** 4358–4370.

Tao, W.-K., and J. Simpson, 1993: The Goddard Cumulus Ensemble model. Part I: Model description. *Terr. Atmos. Oceanic Sci.,* **4,** 35–72.

——, D. Johnson, C.-L. Shie, and J. Simpson, 2004: The atmospheric energy budget and large-scale precipitation efficiency of convective systems during TOGA COARE, GATE, SCSMEX, and ARM: Cloud-resolving model simulations. *J. Atmos. Sci.,* **61,** 2405–2423.

Weisman, M. L., and J. B. Klemp, 1982: The dependence of numerically simulated convective storms on vertical wind shear and buoyancy. *Mon. Wea. Rev.,* **110,** 504–520.

Weller, R. A., and S. P. Anderson, 1996: Surface meteorology and air–sea fluxes in the western equatorial Pacific warm pool during TOGA Coupled Ocean–Atmosphere Response Experiment. *J. Climate,* **9,** 1959–1990.

Wu, X., W. W. Grabowski, and M. W. Moncrieff, 1998: Long-term behavior of cloud systems in TOGA COARE and their interactions with radiative and surface processes. Part I: Two-dimensional modeling study. *J. Atmos. Sci.,* **55,** 2693–2714.

Xu, K.-M., and D. A. Randall, 1996: Explicit simulation of cumulus ensembles with the GATE Phase III data: Comparison with observations. *J. Atmos. Sci.,* **53,** 3710–3736.

Zhang, M. H., and J. L. Lin, 1997: Constrained variational analysis of sounding data based on column-integrated budgets of mass, heat, moisture, and momentum: Approach and application to ARM measurements. *J. Atmos. Sci.,* **54,** 1503–1524.